The Influence of Creep on the Failure of Wood-framed Walls in Fire

PAUL CLANCY* AND FRANCISCO JONG

CESARE, Victoria University of Technology,
P.O. Box 14428, Melbourne City,
MC 8001, Australia

ABSTRACT: Elastic models for wood-framed walls in fire have been developed following the advent of performance-based regulations. The main problems include the modeling of walls with high load ratios and large differences between elastic moduli obtained by direct measurement and by calibration of models to full scale wall tests. Described in this paper are models for creep of wood which have been incorporated into an elastic wall frame model to produce creep models for walls. These models are used to explain anomalies and overcome these problems. Limitations to elastic models and evidence for mechano-sorptive creep caused by changes in moisture are given.

KEY WORDS: wood, wall, elasticity, creep, fire resistance, model.

INTRODUCTION

THE ADVENT OF performance-based fire safety regulations in countries around the world has led to the development of models to demonstrate compliance of innovative building practices. Opportunities are available to overcome the prohibitive restrictions against timber by traditional prescriptive regulations. To realize some of these opportunities, structural models [1–9] have been developed to predict the behavior of wood-framed walls in fire. These structural models mainly have used elastic theory, which is probably the most widely used theory in structural engineering. In elastic theory, the load resistance is proportional to deformation until failure

*Author to whom correspondence should be addressed. E-mail: Paul.Clancy@vu.edu.au

1042-3915/03/04 0221–30 $10.00/0 DOI: 10.1177/104239103033493

occurs by either rupture or buckling. The main variables in elastic theory are the elastic modulus and strength.

For a number of comparisons between modeling predictions and experimental results, elastic theory appears to have worked well – although there have often been large differences between the mechanical properties used by modelers to model full scale walls and the mechanical properties obtained from independent small scale experiments [4,6,11]. It is believed that many of these differences can be attributed to creep.

A full-scale wall was exposed to a standard fire [4,6] which resulted in failure that could not be explained with elastic theory. The wall was 3 m high, was supported with pinned ends and comprised studs 90 mm × 45 mm in section each subjected to a vertical load of 8 kN. The studs did not break but rather bent as though they were partly plastic. The studs were not totally plastic because failure was not sudden. A low level of structural resistance continued. The average temperature of wood in the studs was approximately 100°C. There was little or no charring. It is believed that creep had a large role in the failure of the full-scale wall experiment. The results from this experiment are of concern, because one elastic model [7] has been largely used in the development of the Eurocode and another [1,2] is widely used in industry practice in Australia and New Zealand. Since it is intended to use these and other elastic models to predict the behavior of walls beyond sizes that can be tested with furnaces, it is necessary that the limitations of elastic modeling be found. The elastic models have been evaluated intensively with much furnace testing and thus it is unlikely that there will be a serious failure. However, the safe limits to the use of these models must be known.

Experimental research was undertaken to measure creep properties of wood in compression and has been reported previously [12,13]. Equivalent elastic and empirical wood creep models were deduced. The equivalent elastic model used reduced elastic moduli to allow for creep strains and is valid for a limited range of conditions. The empirical creep model gives a mathematical expression for creep involving coefficients which are functions of moisture content, stress, temperature and time.

The aim of the research described in this paper was to incorporate the equivalent elastic and wood creep models into an existing elastic wall model to produce new creep models for walls. These new models with various modifications were used to evaluate whether the problems with mechanical properties and the elastic modeling of the full-scale wall could be explained with creep. Several consequences of creep on the behavior of walls in fire are discussed subsequently.

SUMMARY OF CREEP EXPERIMENTS AND WOOD CREEP MODEL

Experiments were undertaken [12,13] to determine creep in different regimes of temperature, moisture and load. These regimes were:

1. 20–100°C, moisture contents of 12 and 30%, and loads of approximately 6 and 8 MPa.
2. 20–100°C, specimens with 0% moisture content, and a load of approximately 8 MPa.
3. 150–250°C, specimens with 0% moisture content, and load of approximately 8 MPa.
4. 100°C, moisture content reducing below 30% with time, and 8 MPa load.

The above regimes cover the full range of conditions experienced by wood in fire. Temperatures in wood in fire are below 300°C because above this temperature wood only exists in the form of char. The fiber saturation level in wood is 30%. Higher moisture contents are possible but involve moisture being stored in the pores instead of the wood fiber. Compared with wood at 30% moisture content, higher moisture contents do not significantly affect mechanical properties. The moisture content of 12% is the approximate value for seasoned radiata pine which is the most commonly used species of wood used in building construction in Australia. It appears that the corresponding moisture content for spruce commonly used in North America and Europe is 10% [10]. The moisture content of 0% was obtained by slow oven drying at marginally above 100°C. Thus moisture contents covered the full range expected for wood. A typical load on a 90 mm × 45 mm stud in service conditions is approximately 8 kN [4] or an average compression stress of 2 MPa. Testing to a load of 6–8 MPa will thus be more than most loads expected in service.

All of the specimens in the experiments were radiata pine. They were cut to a size of 300 mm in length by 90 mm × 35 mm in cross-section.

Regimes 1 and 4 involved the placement of specimens in a tank of water at constant temperature. The specimens were cut with tapers near the ends so that the middle half was 30 mm × 35 mm in section, as shown in Figure 1. The tapers prevented bearing failure at the ends. The moisture content of 12% was maintained by painting specimens with three coats of acrylic paint. The specimens with a moisture content of 30% were exposed directly to the water. Since the moisture content of these specimens was at the fiber saturation level, the moisture content in the wood fiber would not have been affected by direct exposure to water. The water helped to ensure that the moisture contents in wood specimens were approximately constant at temperatures approaching 100°C. The moisture content was checked for

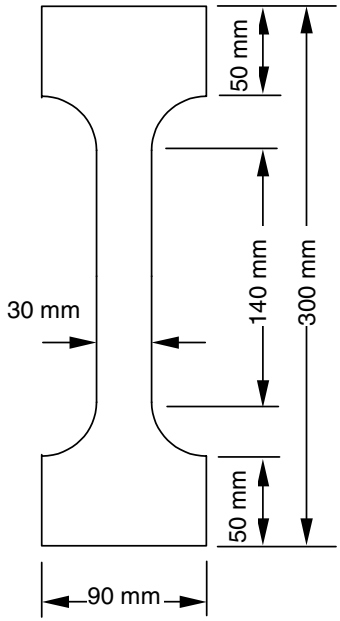

Figure 1. *Dimensions of specimens used in creep experiments.*

constancy by weighing. The water also enabled specimens to be heated to elevated temperatures in a similar period of time as for studs in wood-framed walls in fires. The purpose of regime 4 was to investigate mechano-sorptive creep. This type of creep depends on the change in moisture rather than the actual moisture content.

Regimes 2 and 3 involved heating specimens with steel plates while in a compression testing machine in, otherwise, ordinary atmospheric conditions. The heating procedure with steel plates has been fully described previously [11]. The plates were loosened to ensure that compression resistance of the specimens was not assisted by lateral support. Such assistance can be caused by the Poisson effect.

It is difficult to devise experiments that will clearly indicate mechano-sorptive creep because of the long period of time for wood specimens to dry. The drying process in wood studs in fire only occurs over widths of a few millimeters during periods of several minutes. Such small widths in isolation are difficult to load in compression. The experiments undertaken to evaluate mechano-sorptive creep did not reveal any that was discernable.

The elastic moduli were deduced in the initial stages of loading as indicated in Figure 2. The load versus deflection was plotted. The steepest

tangent was obtained soon after loading commenced when the load fully engaged the specimen. The tangent modulus was used to remove all effects of creep from the deduced elastic modulus. This procedure differs from conventional determinations of elastic modulus which involve a specified strain rate [14] indicated by the ASTM plot. Elastic moduli were determined relative to the elastic modulus of radiata pine at 12% moisture content at ambient conditions.

The relative elastic moduli for radiata pine with moisture contents of 0, 12 and 30% are plotted in Figure 3 [12,13]. The relative moduli are taken relative to the elastic modulus for the conditions of ambient temperature and a typical moisture content of 12%. The plots for 12 and 30% do not extend above 100°C because wood above the vaporization point should be approaching a dry state. The temperature of 100°C was determined to be the vaporization point from observation of the dwell in temperatures measured with thermocouples. It has been shown [15,16] that, as the temperature at a particular position in wood approaches the vaporization point of moisture in the wood, the moisture content at that position approximately doubles. The reason is that the pressures created by vaporization move vapor into regions at lower temperatures where condensation then takes place. Allowing for the expected doubling of moisture content from 12% at ambient conditions to 24% at the vaporization point, a plot of the relative elastic modulus with temperature expected for wood typically used for studs and other light framing, should decrease to a relative modulus of 0.40. As temperature increases further, moisture should decrease due to vaporization and the relative elastic modulus should approach values for 0% moisture

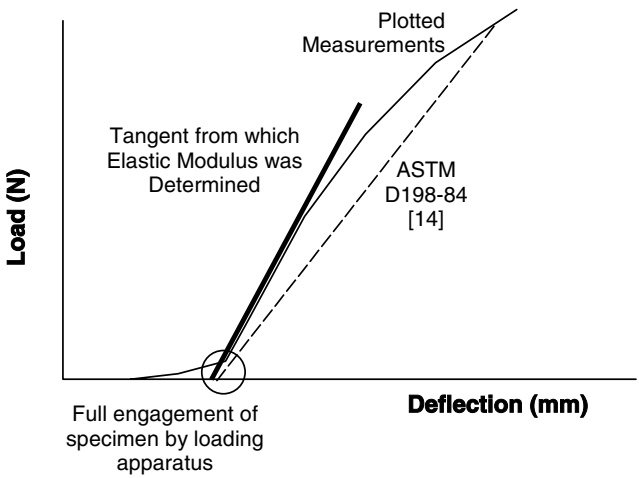

Figure 2. *Graphical approach for determining the elastic modulus of wood in compression.*

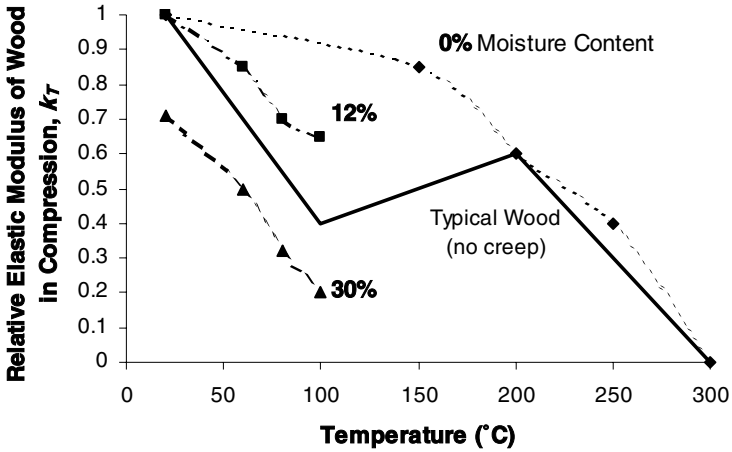

Figure 3. *Relative elastic modulus of wood in compression.*

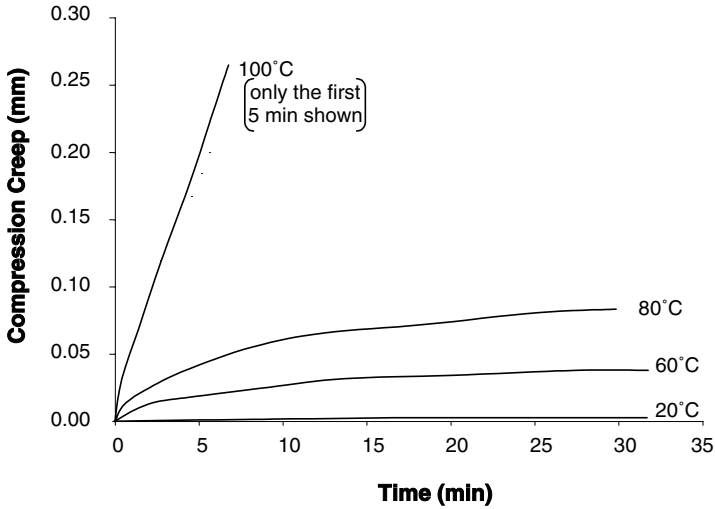

Figure 4. *Example of results from compression creep experiment involving specimen with 30% moisture content and 8 MPa loading.*

content, dry wood. It is assumed that 0% moisture content occurs at the approximate temperature of 200°C. Thereafter, the relative elastic modulus should decrease to zero at approximately 300°C when wood turns to char.

Examples of plots of measured creep deflections with time are shown in Figure 4. These examples are for wood with a moisture content of 30% and a load of approximately 8 MPa. The measured deflections were taken over a

gauge length of 100 mm at the center of the specimens. Only the first five minutes of the plot for 100°C is shown so that the differences between plots for other temperatures can be observed. The steep plot for the specimens at 100°C indicates that the strength of the wood apparently reduced close to the value of the load applied and the wood was approaching a plastic state.

A wood creep model was obtained empirically by calibrating coefficients A and B in the following general equation for creep, ε_{cT}, to plots such as those in Figure 4 [13].

$$\varepsilon_{cT} = At^{B}\varepsilon_{eT} \tag{1}$$

where ε_{eT} is the elastic strain of wood at temperature, T; t is the time (min); A is the coefficient listed in Tables 1 and 2; B is the coefficient listed in Tables 1 and 2.

The elastic strain, ε_{eT}, is obtained from,

$$\varepsilon_{eT} = \frac{\sigma}{k_T E_{20}} \tag{2}$$

Table 1. Creep coefficients for temperatures between 20 and 100°C.

Moisture Content (%)	Elastic Strain in Wood at 20°C	20°C		60°C		80°C		100°C	
		A	*B*	*A*	*B*	*A*	*B*	*A*	*B*
0	all strains	0	0	0	0	0	0	0	0
12		($k_T = 1.00$)		($k_T = 0.85$)		($k_T = 0.70$)		($k_T = 0.65$)	
	0	0	0	0	0	0	0	0	0
	0.000408	0	0	0.167	0.312	0.185	0.387	0.321	0.252
	0.000544	0	0	0.222	0.312	0.246	0.387	0.429	0.252
30		($k_T = 0.71$)		($k_T = 0.50$)		($k_T = 0.32$)		($k_T = 0.20$)	
	0	0	0	0	0	0	0	0	0
	0.000571	0	0	0.077	0.511	0.445	0.199	0.469	0.387
	0.000762	0	0	0.141	0.387	0.267	0.421	0.332	1.285

Table 2. Creep coefficients for temperatures between 150 and 300°C.

150°C ($k_T = 0.85$)		200°C ($k_T = 0.60$)		250°C ($k_T = 0.40$)		300°C ($k_T = 0.00$)	
A	*B*	*A*	*B*	*A*	*B*	*A*	*B*
0.289	0.473	0.370	0.613	0.664	1.285	failure	

where σ is the compressive stress (MPa); k_T is the relative elastic modulus of wood in compression at temperature T, obtained from Figure 3; E_{20} is the elastic modulus of wood in compression at an ambient temperature of 20°C and a moisture content of 12% (MPa).

The variables, ε_{eT} k_T E_{20}, are all for the same moisture content.

The coefficients A and B in Tables 1 and 2 are given for the elastic strain at 20°C, ε_{e20}, that would involve the same load resistance corresponding to the elastic strain at the temperature in question. The elastic strain at 20°C, corresponding to some known elastic strain at temperature T in a computer model, can be found from the equation,

$$\varepsilon_{e20} = k_T \cdot \varepsilon_{eT} \tag{3}$$

Values for A and B are obtained in the explicit creep model described below, by interpolation, for loads, temperatures and moisture contents within the bounds of Tables 1 and 2.

SUMMARY OF EXISTING ELASTIC WALL MODEL

The existing elastic wall model, that was used as the basis for developing new creep models for walls, was developed by Young [6,9]. This model was appropriate for including creep because of its constitutive analytical approach which involves the direct modeling of materials. The model predicts the overall structural behavior of a wood-framed wall from the specified axial behavior of small discrete elements in wood and gypsum board. Young's model was modified by simply including relationships for creep with the elastic relationships that he specified for the axial behavior of the elements. Creep strains increase the overall deflections while the load resistance remains a function of the elastic strain alone. Young's elastic wall model is subsequently summarized in more detail.

Discretization of Wall Cross-section into Elements

Young's model [9] was developed for walls and floors comprising parallel studs (or joists) with sheeting such as gypsum board on one or both sides, and no cavity insulation as shown in Figure 5. The model allows for any amount of rotational support stiffness ranging between pinned and fixed conditions. It analyzes a single stud and its tributary sheeting as an equivalent line member comprising nodes and discrete segments.

A section through a typical segment is shown in Figure 6. The section is discretized into a grid of elements each of which is assumed to behave as an elastic spring. Elements act fully compositely in the stud and fully

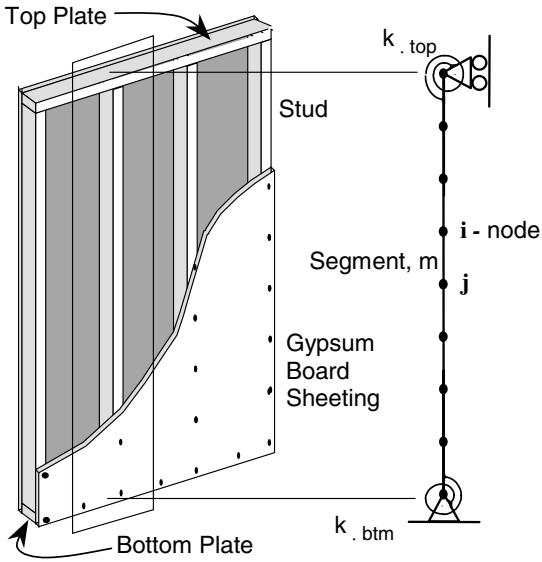

Figure 5. *Discretization of wall frame into segments [6].*

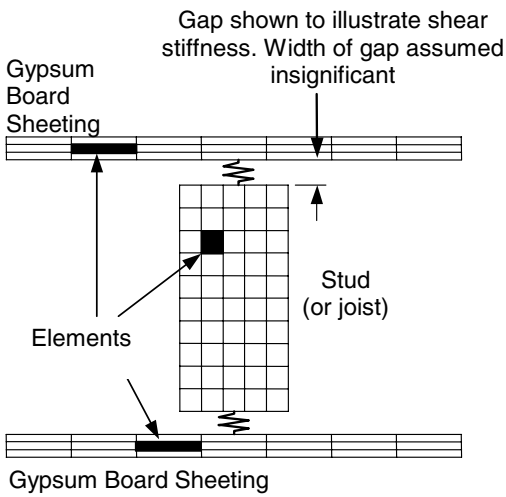

Figure 6. *Discretization of a member segment into elements [9].*

compositely in the sheeting; that is, without relative slip between elements. The sheets and the stud are assumed to act in partial composite action which is modeled with slip resisted by shear springs representing the actions of fasteners such as nails or screws.

Incorporation of Elements into Second Order Frame Analysis

The model incorporates the discrete elements into a frame analysis of a wall as shown in the flowchart in Figure 7. In box 3, the stiffness for discrete elements is combined using composite theory to obtain the stiffness for vertical segments of the wall shown in Figure 5. The stiffness for the segments is combined using second order frame analysis. As a wall frame deflects under vertical load, the stiffness in terms of vertical load resistance

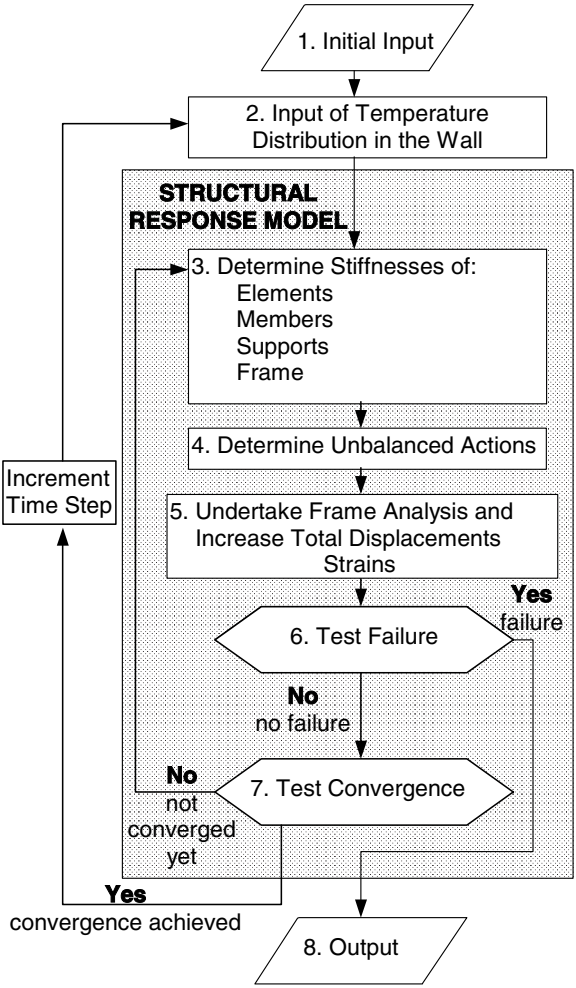

Figure 7. *Flowchart showing overview of structural response model [9].*

per unit deflection is reduced. The greater the bow in the wall (curvature of the deflected shape), the more the wall must deflect and the less stiffness the wall has to support the same load. When there is little or no compression, this reduction is negligible and a first order analysis can be used effectively based on the initial shape prior to deflection. The model undertakes second order analysis in the repeated execution of the loop involving Boxes 3–7. In each execution, Box 4 determines the load resistance based on the member stiffness determined from the latest computed deflected shape. The load resistance of the deflected wall is a little less than the applied load. The difference is termed the unbalanced load which is computed and reapplied to the stud. The loop is repeated until the unbalanced load actually fails the stud (Box 6) or convergence is achieved with an acceptably small unbalanced load (Box 7). Failure involves either insufficient strength of the member cross-section or buckling. For a particular temperature distribution, strength of the equivalent member reduces with the removal of discrete elements that are stressed beyond their strengths. Buckling is predicted from numerical divergence in which the unbalanced load increases with each execution of the loop, Boxes 3–7.

Incorporation of Second Order Frame Analysis into Thermal Analysis

Upon convergence of the unbalanced load, the deflections are recorded and the model advances to the next time step. Temperatures in the discrete elements are updated with the use of models for fire severity and heat transfer (Box 2). The structural response of the wall at the new time step is determined with a new iteration of the loop involving Boxes 3–7. In the iteration, higher temperatures lead to lower stiffness and strength for the elements and the overall wall. The wall deflects further to resist the same load. The model proceeds with further time steps until failure is predicted, at which stage the time-to-failure is recorded.

EQUIVALENT ELASTIC MODEL (IMPLICIT CREEP)

The most simple method for modeling creep is to use an equivalent elastic modulus in elastic models such as Young's [6,9]. Equivalent elastic moduli can be predetermined so that predicted deflections are similar to the total measured deflection which includes both creep and elastic behavior. Equivalent elastic moduli cannot be used to model all of the dominant variables in creep – stress, time, moisture content and temperature. The moduli should be based on a limited typical range of values for these variables. Although the use of equivalent elastic models is limited, it is nonetheless practical.

Approximate equivalent elastic moduli for wood at elevated temperatures were derived in previous research [12,13] from the creep experiments summarized earlier in this paper. The elastic and creep deflection measurements were found to be similar for the wood specimens loaded for a period of 30 min at 100°C. It is believed that this similarity between creep and elastic deflection commonly applies because the specimens had a typical initial moisture content of 12% and the size of 300 mm × 95 mm × 35 mm was substantial. The plot for the equivalent elastic modulus expressed in terms of k_T, which is the relative value compared to the modulus at 20°C, thus passes through D, in Figure 8. At this point, corresponding to a temperature of 100°C, the variable k_T is 0.20 which is half the value for the elastic modulus at 100°C. The research also involved measurements of creep at temperatures between 150 and 250°C (refer to regime 3 and Table 2). The creep was substantial. Considering the approximate nature of the equivalent elastic modulus it was decided to reduce k_T linearly from a value of 0.20 at 100°C through 0.00 at 300°C. The equivalent elastic modulus that was derived in Figure 8 was derived for the following limitations – wood enduring constant temperature, stress and moisture for 30 min.

Plots of elastic moduli for wood in compression published by other researchers are shown in Figure 9. Plots by König and Walleij [7], Young and Clancy [11] and Thomas [3] are the most similar to the equivalent modulus. This similarity is expected since these researchers obtained their plots by calibrating models to results of wall behavior in full-scale furnace experiments. Plots by Gerhards [18] and White et al. [17] are very different. Their plots were obtained directly from load-deflection measurements of

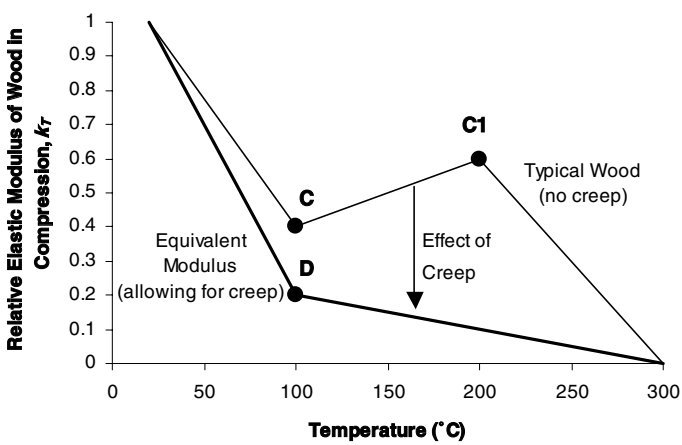

Figure 8. *Equivalent elastic modulus of wood in compression, allowing for creep.*

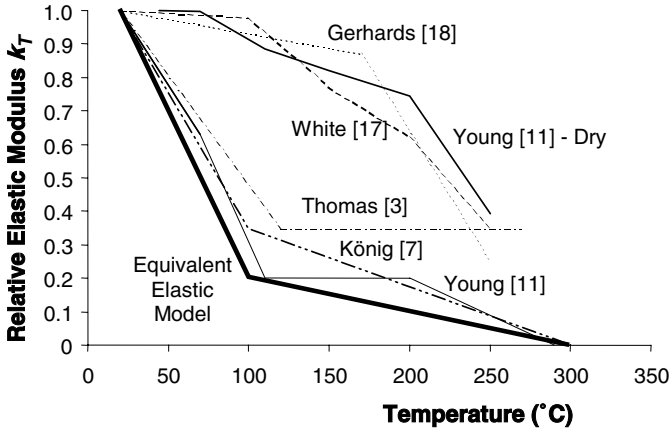

Figure 9. *Summary of relative elastic moduli for wood given in the literature.*

specimens in compression. It appears that their high values of the elastic modulus were due to the use of small specimens that dried quickly when heated. Drying increases the elastic modulus. As well, they used fast loading rates that eliminated creep.

The equivalent elastic approach is most likely to be adopted by designers in preference to more complex methods. However, the safe limits for using equivalent elastic moduli need to be determined with explicit modeling which involves more direct modeling of creep.

EXPLICIT CREEP MODEL

The explicit model involves the direct calculation of creep strain as a function of all the dominant variables – temperature, stress, moisture content and time. This direct calculation was undertaken for each small discrete wood element in Young's model. Any creep of the gypsum board was ignored. Each discrete element is assumed to have uniform temperature and material properties. The total strain, ε_{tot}, in a wood element is given by the equation,

$$\varepsilon_{\text{tot}} = \varepsilon_e + \varepsilon_c \tag{4}$$

The creep strain is determined in accordance with Equation (1). Thermal strains are ignored because wood has a very low coefficient of thermal expansion. Elastic and creep strains are very much larger than thermal strains.

The modeling of these components of strain, ε_{e} and ε_{c}, in a discrete element is illustrated in Figure 10. The elastic behavior is represented with

springs and creep behavior is represented with dashpots. The modeling of the structural behavior of elements involved repeated numerical simulations in many time steps during the period of fire exposure. The simulations involved the following sequence in each time step:

1. At the beginning of a time step, t_i, in Figure 10(b), the load resistance of an element is equal to the total applied load, P_{tot} and the total strain is ε_{tot}.
2. During the time step creep is simulated assuming that the mechanical properties as well as total strains remain constant. Creep is indirectly modeled using relaxation and thus overall deflections do not change. The load resistance reduces as the element relaxes with time. The spring lengthens and the dashpot compresses as shown in Figure 10(c). Elastic strain in the element reduces by the same amount that the creep strain increases, $\delta\varepsilon_c$, such that the total strain, ε_{tot}, is maintained constant during the current time step. Since the elastic stiffness provides the load resistance, the resistance is less than the applied load. The difference is referred to as unbalanced load.
3. The loss of load resistance due to thermal degradation of the elastic moduli of elements and due to failure of elements stressed beyond

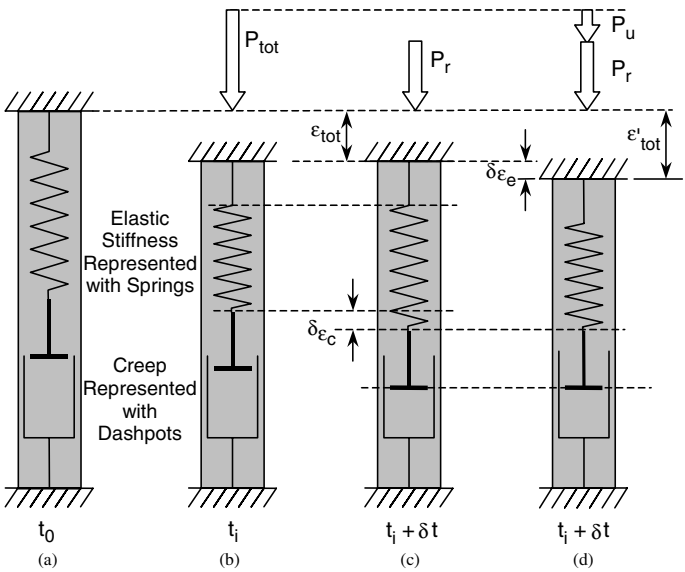

Figure 10. *Incorporation of creep into modeling of compression of element. (a) Initial unloaded element; (b) At beginning of current time step; (c) Completion of relaxation towards end of time step; (d) Application of unbalanced load at end of time step.*

their capacity is determined at the end of the time step. These losses create further unbalanced loads. The total unbalanced load is denoted as P_u.

4. At the end of the time step, P_u is applied as shown in Figure 10(d). The element is assumed to respond elastically and instantaneously. The total strain increases to ε'_{tot}. The increase in the total strain is the same as the increase in the elastic strains, $\delta\varepsilon_e$. The corresponding overall deflections of the wall increase. The unbalanced load is not actually applied to individual elements but rather to nodes shown in Figure 5. A node is at the centroid of a cross-section. Since elements are some horizontal distance from a node, force and moment that is statically equivalent to the unbalanced load is applied at the node. The conventional assumption associated with full composite action, that plane sections remain plane, is applied within each sheet and in the member. Adjacent elements in sheets or the member do not slip against each other.

The creep coefficients listed in Tables 1 and 2 apply for constant load (MPa), temperature and moisture content. Obviously, values for these variables will change during fire exposure. The method for determining creep strain during a time step is illustrated in Figure 11. It is assumed that creep strain increases in accordance with Equation (1) with coefficients A and B appropriate for the values for variables in the current time step. To determine the increase, the time at which creep at the beginning of the new time step equals the creep at the end of the previous time must be determined. That is, the values of t_1, t_2 and t_3 in Figure 11. Generically,

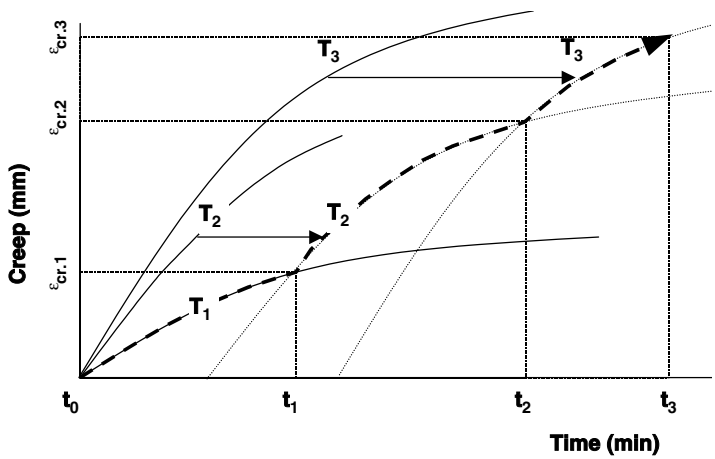

Figure 11. *Calculation of creep involving changes in temperature.*

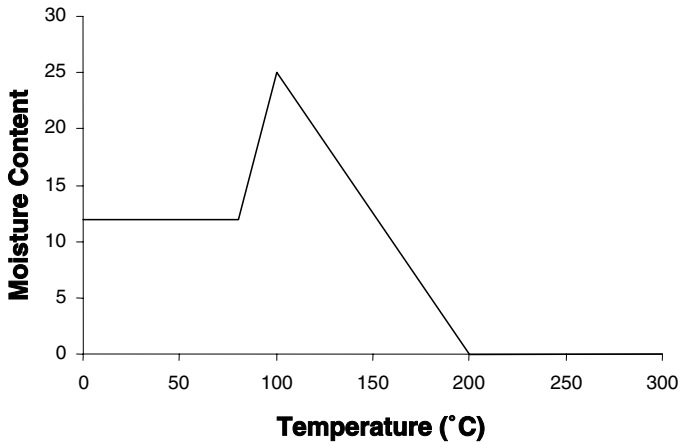

Figure 12. *Assumed relationship between moisture content and temperature in wood.*

these times are denoted as t_c. By rearranging Equation (1) t_c is found as follows.

$$t_c = \left(\frac{\varepsilon_{ci}}{A_{i+1}\varepsilon_{ei}}\right)^{1/B_{i+1}} \tag{5}$$

Creep at the end of the new time step, t_{i+1}, is thus,

$$\varepsilon_{c.i+1} = A_{i+1}(t_c + \delta t)^{B_{i+1}} \tag{6}$$

Since moisture contents, which are required by the creep model, are seldom measured or predicted in available thermal analyses, the relationship between moisture content and temperature in wood shown in Figure 12 was adopted. Moisture measurements [15,16] in slabs of wood exposed to standard fire, were used as a guide for deducing the proposed relationship. A moisture content of 12% applies to seasoned wood between 0 and 80°C. This moisture content doubles in the region of vaporization. By 200°C it is assumed that all moisture has vaporized leaving the wood dry.

ALTERNATIVE MODIFICATIONS TO MODELS

To enable the evaluation of the effects of the different variables on creep several modeling modifications were considered. The explicit creep model described previously is referred to as the *basic creep model*.

As previously explained for the creep experiments, creep of wood is not only a function of the absolute moisture content but also of the change in moisture content. Reductions in moisture content (desorption) cause more creep than increases (adsorption). Creep due to the change in moisture content is termed mechano-sorptive creep. The basic creep model was modified for this type of creep and is referred to in this paper as the *creep model modified for mechano-sorption*. Modification for mechano-sorptive creep was undertaken by preventing any reduction in the magnitude of strain determined numerically in a discrete element unless there was a reversal of stress from compression to tension or vice-versa.

Coefficient A was also obtained by calibration of the explicit model to the results of the full-scale furnace experiment involving a wall with fixed-end supports which is described as wall Experiment 1 later in this paper. The resulting calibration resulted in all coefficients A in Tables 1 and 2 being scaled by a factor of 2.5. The calibration led to the modification referred to as the *calibrated creep model*. The factor of 2.5 was used in the evaluation of calibrated creep model predictions against all experimental results described in this paper. Coefficient B was not calibrated for several reasons. Since B is an exponent, a small change in B will greatly affect the curvature of the plot of creep deflection with time. After having undertaken many creep tests, it was believed that the basic shape of the plots was accurate. It was thought that if there were any inaccuracies in measurements, they would be limited to scale effects which are represented in coefficient A. Furthermore, since the knowledge of creep of wood in fire is not highly advanced, it does not appear warranted to attempt the level of refinement in calibrating both coefficients A and B. The experiment on a wall with fixed-ends was chosen as the basis for calibration because it was felt that this type of wall is used much more often than the alternative of pin-ended walls. Calibration for a wall without cavity insulation rather than with cavity insulation was chosen because the studs in an uninsulated wall would heat more quickly and thus provide clearer evidence of creep.

The alternative elastic models that were evaluated were the *elastic model* which used the elastic modulus associated with the plot through points C and C1 in Figure 8, and the *equivalent elastic model* which used the elastic modulus associated with the plot through point D in the same figure.

EVALUATION OF MODELS AND THE INFLUENCE OF CREEP ON TIME-TO-FAILURE

Evaluations of models involved comparisons with results from three wall experiments undertaken previously. The walls had different cross-sections and were exposed to different fires. The first evaluation was undertaken for

a wall that had fixed-ends, hollow cavities [6] and was exposed to standard fire [19]. The second evaluation was undertaken for two walls that were similar to the first except they had pinned-ends [6]. The third evaluation was for a wall that had insulated cavities, fixed-ends and was exposed to a parametric realistic fire [7]. For all of the walls, measurements [6,7] of temperatures at points throughout stud sections were available and were input directly into the creep model. Thus little error could be attributed to thermal modeling and the performance of the structural modeling could be appraised confidently. Mechanical properties used in the evaluation of the three walls, and not described in this paper, were adopted from previous research [6,11].

Wall Experiment 1 – Fixed-ended Hollow Cavity Walls in Standard Fire

Only one fixed-ended wall was tested because, previously in the experimental program, times-to-failure for similar walls were reproduced closely – within one minute of each other. The experiment was designed with well known boundary conditions including support fixity and heating conditions. The top and bottom plates were fixed against translation and rotation by screwing the plates to steel supports. The studs were connected to the plates with skew nailing. There were no other restraints to provide lateral support to the wall. The wall comprised five 90 mm × 45 mm radiata pine studs spaced 380 mm between centers. The studs had an average initial moisture content of 12%. The outer two studs were cut in several places and were not structural. Their purpose was to provide blocking to any heat transfer through the vertical edges of the wall and thus ensure that all load bearing studs thermally degraded in a similar known manner. Each of these studs was loaded with 8 kN applied at a 10 mm eccentricity towards the fire. The reasons for the eccentricity were to simulate realistic loads which are eccentric, and to add to normal deflections which, for wood-framed walls, are directed out from the fire. The load of 8 kN created an average axial stress of approximately 2 MPa which is within the range of variables in Tables 1 and 2. The studs were sheeted each side with 16 mm thick fire-rated gypsum board (810 kg m^{-3}). The gypsum board was fastened to the wood framing with nails that were 50 mm long and 2.8 mm in diameter. Around the perimeter of each board the nails were placed 100 mm on center. Elsewhere along studs and blocking the nails were in pairs spaced at 300 mm on center. This construction, except for the outer studs being cut, had a standard fire rating of 60 min in accordance with ISO834.

The thermocouples, for obtaining the temperature distributions in the wood, were placed in blocks of wood. The blocks were similar to the studs except were only 380 mm long and were placed in cavities.

The thermocouples were placed in the blocks rather than the studs to avoid interfering with the structural resistance of the studs. The thermocouples were arranged so that their ends were arranged in a grid to enable two dimensional temperature distributions to be obtained accurately by interpolation.

Predicted and measured deflections of the fixed-ended wall are plotted in Figure 13. The deflections in the last minutes increase dramatically. To enable some detail to be observed during the first 50 min of the plots and to avoid congestion, the last 1–2 min of the plots have been truncated. Reading the ends of the plots from right to left on the figure, the following observations are made:

1. Using elastic modeling the predicted time-to-failure (Elastic) is 70 min which exceeds the observed time-to-failure of 59 min corresponding to the plot marked "Test".
2. Using the basic creep model and the relationship for moisture content versus temperature in Figure 12, the predicted time-to-failure (Creep 1) was 66 min. In some cases it may be possible for deflections to reduce as wood temperatures rise above 100°C because the elastic modulus is

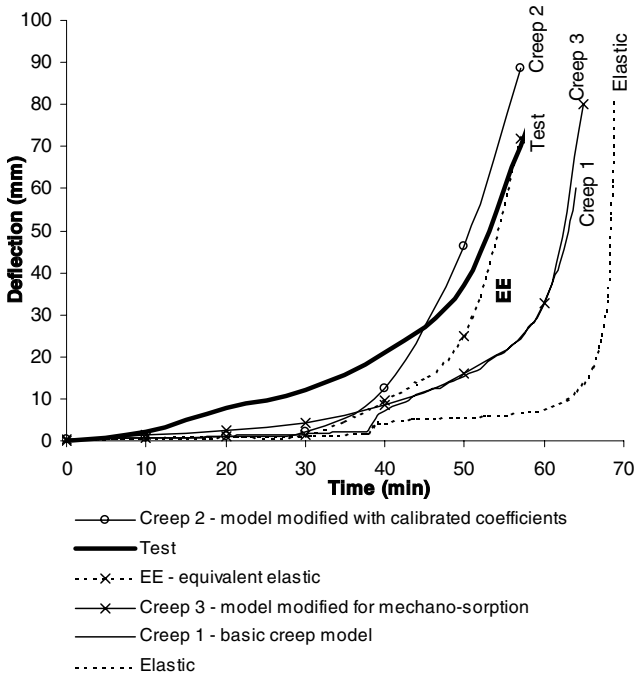

Figure 13. *Deflections of fixed-ended wall vs. time.*

expected to rise towards point C1 in the plot in Figure 8. However, a reduction in deflection at this stage was not predicted with the basic creep model. Apparently, the increase in creep deflections exceeded the reduction in elastic deflections.

3. The predicted time-to-failure (Creep 3) using the creep model modified for mechano-sorption was approximately the same as for the basic creep model (Creep 1). This result is expected following the previous observation that deflections predicted with the basic creep model did not decrease as the elastic modulus increased with temperatures above 100°C. Since deflections did not decrease, strains did not decrease and the mechano-sorption algorithm that prevents reductions in strains was not applied.
4. For the equivalent elastic model the predicted time-to-failure (EE) was 58 min.
5. As mentioned above, the observed time-to-failure in the test was 59 min. This time is less than the fire rating of 60 min because in a standard wall the outer studs are not cut and do provide the additional fire resistance to increase the rating above 60 min.
6. As would be expected with calibration, the calibrated creep model predicted the same time-to-failure (Creep 2) as observed in the experiment.

The three plots for explicit creep modeling (Creeps 1–3) are approximately gathered around the plot for the test. In comparison, the plot for elastic modeling (Elastic) is further to the right, indicating greater stiffness. The creep modeling used the same elastic modulus, shown as the plot through C–C1 in Figure 8, as was used in the elastic modeling. Plot C–C1 is considerably higher than the calibrated plots obtained by Thomas [3], König and Walleij [7] and Young and Clancy [11]. It is similar to Gerhards' [18] and White et al.'s [17] plots in the dry region (temperature greater than 200°C) obtained by measurement. Similarity for temperatures less than 200°C cannot be expected because Gerhards and White effectively used dry wood, whereas the wood in the wall experiment was moist for these temperatures. Since the creep plots were derived from measured elastic moduli (the entire plot from 20 to 300°C through C–C1 in Figure 8), the plots demonstrate that creep can be used to reconcile the large difference between measured and calibrated values for the elastic modulus of wood in compression. Calibration has been based on total deformation which not only includes elastic deformation but also creep. Direct measurements to obtain elastic moduli appear to have unwittingly excluded creep.

The time-to-failure is insensitive to creep coefficient A because increasing A by a very large amount, a factor of 2.5 or an increase of 150%, only

reduced the time-to-failure from 66 to 59 min, a decrease of 11%. However, this period of time is significant and hence creep does significantly affect the time-to-failure. The average temperature in uncharred wood at the time of failure was approximately 200°C. It is thus apparent that creep in wood above the vaporization point is significant.

The equivalent elastic modulus gives predictions that compare well with the observed time-to-failure in the fixed-ended wall experiment. This comparison supports the use of this simple approach to modeling wood-framed walls in fire.

An aim in developing models is to predict the time-to-failure of walls that are outside the range of conditions and variables that can be tested with available furnaces. For example, it would be desirable to predict the time-to-failure of walls taller than 3.00 or 4.00 m. The creep models were applied to tall walls of various heights and with sections similar to the section of the fixed-ended wall that was tested. The effect of height on the time-to-failure was analyzed for four cases. For each case, the load per stud in a 3.00-m high wall was 8 kN. Defining load ratio as the vertical load divided by the ambient load capacity, this load corresponds to a load ratio of 0.15. The four cases were:

1. Constant load ratio, equivalent elastic modulus.
2. Constant load ratio, calibrated creep model.
3. Case 1 repeated for constant load.
4. Case 2 repeated for constant load.

The results of predictions are plotted in Figure 14. Plot (1,2) shows the predictions for Cases 1 and 2. Only one plot is shown for these two cases

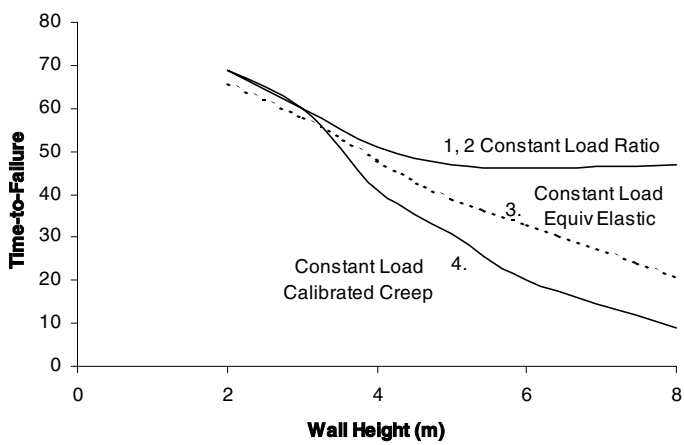

Figure 14. *The effect of wall height on the time-to-failure.*

because the predictions were close, only differing by 0–2 min throughout. It is apparent that the equivalent elastic model, despite ignoring the significant variable of time associated with creep, leads to good predictions compared with predictions of the calibrated creep model. This conclusion is valid for load ratios up to 15% which is typical in wood-framed buildings [4]. Furthermore, it is apparent that for a constant load ratio, the time-to-failure is surprisingly insensitive to height, despite creep. It appears that the time-to-failure is dominated by the time required for heat to penetrate gypsum board. This penetration time is independent of height and creep.

Plots (3) and (4) diverge substantially. This divergence shows that the equivalent elastic model should not be used for high load ratios, above what is normally used in the structural design of buildings. From Figure 15 the maximum acceptable load ratio is 15%.

The effect of creep on the time-to-failure for walls with high load ratios was also predicted for a wall with a constant height of 3.00 m. Again the wall was similar in all respects to the fixed-ended wall, except for the load ratio. Plots of the predictions are shown in Figure 16. For load ratios less than 0.15, the equivalent elastic model gives good predictions compared with the more detailed calibrated creep model. For higher load ratios the equivalent elastic model over-predicts the time-to-failure. Although no further experiments have been undertaken to demonstrate inadequacies in equivalent elastic modeling, potential problems in not modeling creep for load ratios exceeding 0.15 are apparent.

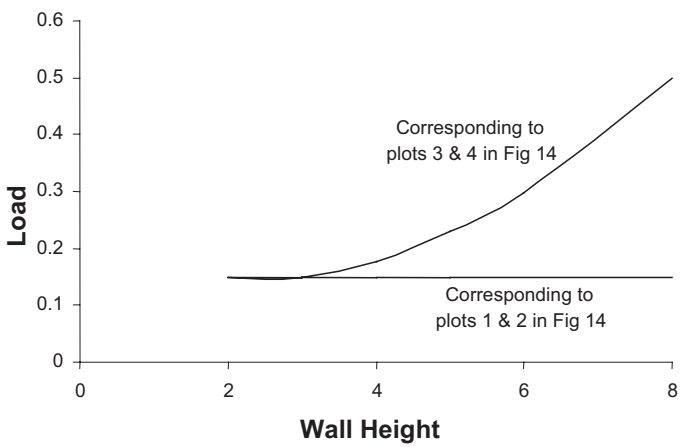

Figure 15. *Load ratios for the plots in Figure 14.*

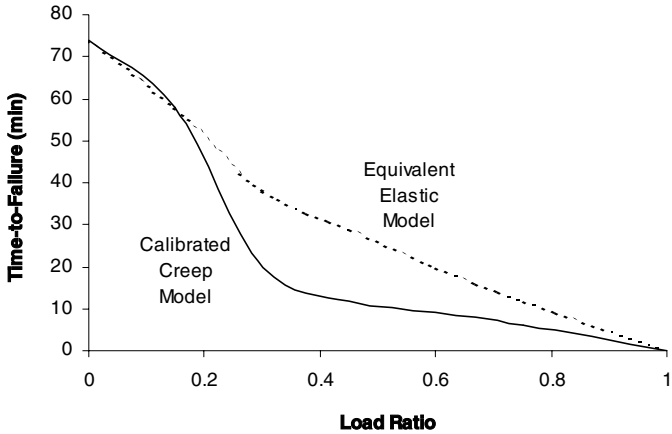

Figure 16. *Effect of modeling assumption on predicted time-to-failure for a wall 3.00 m in height, with different load ratios.*

Wall Experiments 2 – Pin-ended Hollow Cavity Walls in Standard Fire

The pin-ended walls in Experiments 2 were tested similarly to the fixed-ended wall, except the supports were pinned. The pin-ended walls did not behave as would be expected from elastic theory. The temperature of the wood at the time-of-failure averaged approximately 100°C and was within a range 80–110°C. The temperature gradient was low in the stud cross-sections. No rupture of wood fibers was observed in the full-scale experiments at the time-of-failure. The wood had showed characteristics of plastic failure. Failure occurred before any significant charring of the studs commenced.

Predicted and measured deflections of the pin-ended walls are plotted in Figure 17. The last 1–2 min of the plots have been truncated. Reading the ends of the plots from right-to-left on the graph the following observations are made:

1. Using elastic modeling the predicted time-to-failure (Elastic) is 56 min which exceeds the average observed time-to-failure of 35 min corresponding to the plot marked "Test".
2. The time-to-failure predicted with the basic creep model (Creep 1) was 54 min. The plot from the basic creep model was adversely affected by the increase in the elastic modulus after vaporization (segment C–C1 in Figure 8).
3. The creep model modified for mechano-sorptive creep gave a predicted time-to-failure of 40 min (Creep 3). Modeling for mechano-sorption gave

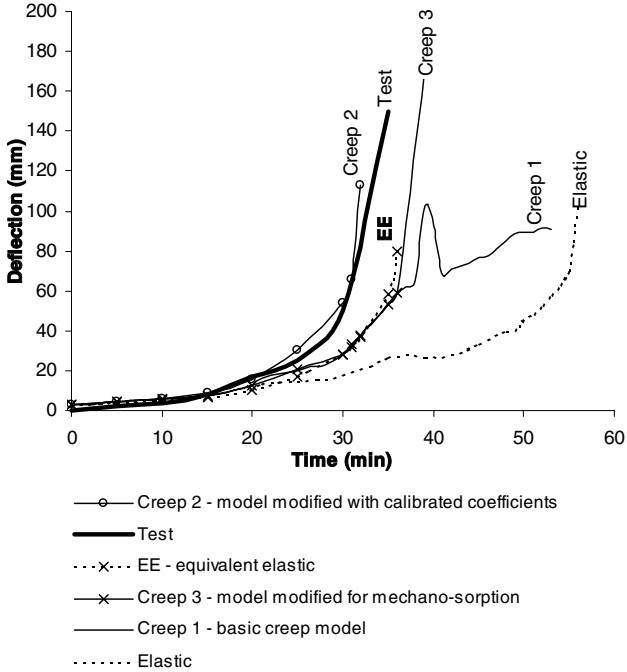

Figure 17. *Deflections of pin-ended wall vs. time.*

a more realistic prediction compared to the prediction with the basic creep model. Evidence is thus apparent for at least some creep being mechano-sorptive in nature.

4. The time-to-failure predicted with the equivalent elastic model was 35 min (EE).
5. The plot for experiment, marked "Test", indicates that the observed time-to-failure was 35 min.
6. The time-to-failure predicted with the calibrated creep model was 33 min (Creep 2).

As explained for wall Experiment 1, comparison of the plots from the creep model modified for mechano-sorption (Creep 3) and the calibrated creep model (Creep 2) compared with the plot obtained from the elastic model (Elastic) can be used to reconcile the large difference between measured and calibrated values for the elastic modulus of wood in compression.

As for wall Experiment 1, large differences in creep coefficients A used to obtain plots Creeps 2 and 3 had a disproportionately small effect on the

time-to-failure. The time-to-failure is insensitive to creep coefficient A. However, comparing the plots labeled Creeps 2 and 3 with the plot labeled Elastic shows that creep substantially affected the time-to-failure.

Once again the equivalent elastic modulus produced surprisingly good results in comparison with the observed times-to-failure.

Wall Experiment 3 – Insulated Wall in Parametric Fire

A typical section through a stud in the wall in the parametric fire experiment, VE14, is shown in Figure 18 [7]. Some of the main details are that the stud was spruce and was 2.5 m tall with a cross-section of 145 mm × 45 mm. The ends of the stud were fixed against rotation and translation. The wall had no lateral support other than at the ends. The load on the stud was 30.3 kN which corresponded to a load ratio of 0.166. The modulus of elasticity was 12,950 MPa. The fire temperature in the furnace was derived [20] from a fuel load of 170 MJ m^{-2} and an opening factor of 0.04 $m^{-0.5}$. The fire temperature was approximately 800°C for the first 30 min and decayed to 250°C by the 120th min.

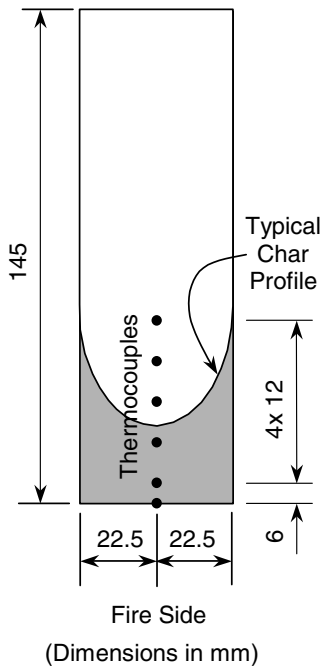

Figure 18. *Instrumented stud in wall in parametric fire experiment.*

Being in an insulated wall, the studs charred from one side. On this side the char profile was rounded.

Thermocouples were inserted along the center line of studs towards the fire side. This arrangement differed to the grids of thermocouples in sections through blocks of wood in wall Experiments 1 and 2. In wall Experiment 3, temperatures in the wood away from the thermocouples were estimated and thus were not as accurately determined as was done by interpolating measured temperatures. Despite lower accuracy, it was still preferable to use measured and estimated temperatures rather than temperatures predicted with heat transfer analysis because of several reasons. The measurements gave temperatures in regions that were most affected by heat. Available heat transfer analyses ignore moisture transfer which is critical to creep.

Predicted and measured deflections of the wall in Experiment 3 are plotted in Figure 19. The last 1–2 min of the plots have been truncated. Reading the ends of the plots from right-to-left on the graph, the following observations are made:

1. The predicted time-to-failure made with the elastic model was 118 min (Elastic).
2. The time-to-failure observed in the experiment was 114 min (Test).

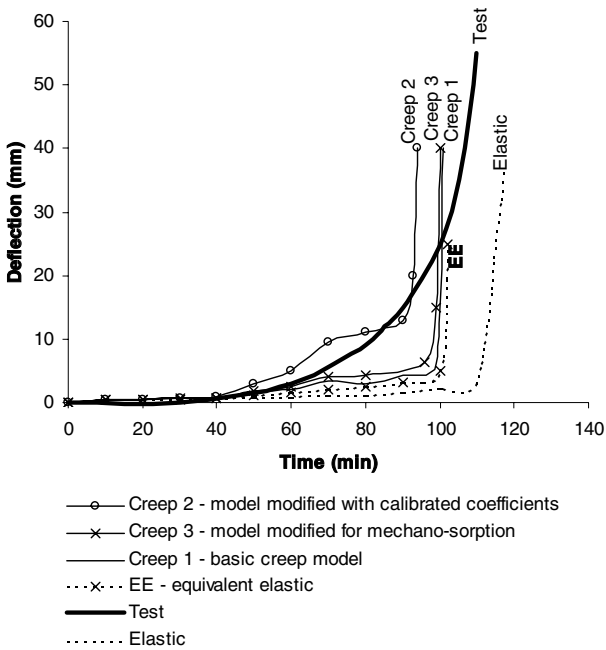

Figure 19. *Deflections of wall VE14 in parametric fire experiment [21].*

3. With the equivalent elastic model, the time-to-failure predicted was 103 min (EE).
4. The time-to-failure predicted with the basic creep model was 102 min (Creep 1).
5. From the creep model modified for mechano-sorption, the time-to-failure was 101 min (Creep 3) which was close to time-to-failure of 102 min for the basic creep model. The effects of mechano-sorption appear to have been minor most likely due to the one-dimensional nature of heat transfer which would have involved steeper temperature gradients compared with gradients from two-dimensional heat transfer in studs in wall Experiments 1 and 2. The steep temperature gradients would lead to only a small proportion of the studs being subjected to changing moisture conditions at any one time, and hence less mechano-sorptive creep.
6. The time-to-failure predicted with the calibrated creep model was 95 min (Creep 2).

Among wall Experiments 1–3, the difference in the times-to-failure for the elastic and equivalent elastic models was smallest in Experiment 3. This small difference can be attributed to the slower one-dimensional heat transfer in the stud in wall Experiment 3 compared with the two-dimensional heat transfer in studs in the other wall experiments. The proportion of stud section being affected by heat would have been least in Experiment 3. Hence the effects of creep would have been least and the differences in the predicted times-to-failure would have been least. The relatively small proportion of section heated in insulated walls makes these walls more amenable to design by net-section analysis. Such analysis involves the adoption of a reduced net rectangular section, which can be analyzed or designed assuming ambient properties.

Predictions for time-to-failure are similar for both the basic creep and equivalent elastic models. These predictions are less than the time-to-failure observed in the experiment and could be due to overestimation of the temperature distributions from the measured temperatures in the studs. The calibrated coefficients in the calibrated creep model did not improve the prediction of the time-to-failure.

The creep did not significantly affect the time-to-failure for a load ratio as high as 0.166. The equivalent elastic model is well supported by the creep analysis. To some extent this conclusion is expected from the slower heat transfer in the studs in insulated walls because a smaller proportion of wood would have been exposed to elevated temperatures which accelerate creep. Since insulated walls creep less than uninsulated walls, equivalent elastic modeling of insulated walls should be valid for higher load ratios than for uninsulated walls.

CONCLUSIONS

Two existing models for creep of wood have been incorporated into an existing elastic wall model to produce creep models for wood-framed walls in fire. The wood creep models include a relationship for an equivalent elastic modulus which predicts the strains that are similar to the total strain which includes both creep and elastic strains. This wood creep model was used to produce an equivalent elastic model for wood-framed walls and is limited in application to typical values for the dominant creep variables; namely, stress, temperature, moisture content and time. Limitations that have been determined include the following. For hollow cavity walls, stress should be limited by ensuring load ratios do not exceed 15%. The initial moisture content for wood should be approximately 12%. For walls with insulation in cavities, the equivalent elastic model can be applied for larger load ratios.

The other wood creep model is an empirical function for creep strain dependent on stress, temperature, moisture content and time. This empirical function was used to produce an explicit basic creep model for wood-framed walls. Several modifications to this basic creep model for walls have been produced. The creep coefficients have been modified by calibration to results from full-scale wall furnace experiments to produce a calibrated creep model for walls. A creep model modified for mechano-sorption ensures that creep strains do not reduce when the magnitude of strain reduces.

The explicit creep models for walls have been used to explain the large differences between elastic moduli for wood compression obtained by calibration and by direct measurement. Calibration has been based on total deformation which not only includes elastic deformation but also creep. Direct measurements to obtain elastic moduli appear to have unwittingly excluded creep.

Although the time-to-failure of wood-framed walls is significantly affected by creep, it is relatively insensitive to the accuracy of creep coefficients that are linear in nature.

Modeling has provided evidence that a significant proportion of the creep in wood in light wood-framed walls in fire is mechano-sorptive in nature.

Despite creep, time-to-failure does not appear to be greatly affected by wall height provided the load ratio is constant and is less than 0.15 which is typical for most wood-framed buildings.

Insulated walls are less susceptible to creep compared with uninsulated walls. It has been shown for one experiment that equivalent elastic modeling can be safely used for load ratios up to one-sixth. Variations in creep coefficients have less effect on the time-to-failure for insulated walls than for uninsulated walls.

NOMENCLATURE

A = creep coefficient listed in Tables 1 and 2
A_{i+1} = creep coefficient A at time step $i+1$
B = creep coefficient listed in Tables 1 and 2
B_{i+1} = creep coefficient B at time step $i+1$
E_{20} = elastic modulus of wood in compression at 20°C (MPa)
k_T = elastic modulus of wood in compression at temperature, T, relative to E_{20}
P_r = load resistance of element (kN)
P_{tot} = total load applied to element (kN)
P_u = unbalanced load (kN)
t_c = time for current creep curve to produce current deflection (min)
t_i = time at current time step (min)
δt_i = increment in time (min)
t_0 = time at beginning of fire exposure (min)
T = temperature (°C)
ε_c = creep strain
ε_{ci} = creep strain at time step i
$\delta\varepsilon_c$ = increase in creep strain
ε_e = elastic strain
ε_{ei} = elastic strain at time step i
ε_{eT} = elastic strain of wood at temperature, T
$\delta\varepsilon_e$ = increase in elastic strain
ε_{tot} = total strain
$\varepsilon'_{\text{tot}}$ = total strain at end of time step
σ = stress (MPa)

REFERENCES

1. Collier, P., *Technical Recommendation N° 9, Design of Light Timber Framed Walls and Floors for Fire Resistance*. BRANZ, August 1991, pp. 17.
2. Collier, P., *A Method to Predict the Fire Resisting Performance of Loadbearing Light Timber Framed Walls*. BRANZ, 1993.
3. Thomas, G.C., *Fire Resistance of Light Timber Framed Walls and Floors*. Fire Engineering Research Report 97/7, School of Engineering, University of Canterbury, Christchurch, New Zealand, 1997.
4. Clancy, P., *Time and Probability of Failure of Timber Framed Walls in Fire*. PhD Thesis, Victoria University of Technology, 1999.
5. Bénichou, N., Sultan, M.A., Takeda, H. and Mehaffey, J.R., "Fire Resistance of Loadbearing Wood-Stud Wall Assemblies: A Tool for Performance Design," 3*rd International Conference on Fire Research and Engineering*, Chicago, USA, 1999.
6. Young, S.A., *Structural Modelling of Plasterboard Clad, Light-Timber Framed Walls in Fire*. PhD Thesis, Victoria University of Technology, 2000.

7. König, J. and Walleij, L., *Timber Frame Assemblies Exposed to Standard and Parametric Fires, Part 2: A Design Model for Standard Fire Exposure*. Trätek (Swedish Institute for Wood Technology Research), Stockholm, Report I 0001001, 2000.
8. Nicholls, K. and Carne, D., *A Structural Design Methodology for Lined Timber Stud Walls Exposed to Fire Regime Defined by AS* 1530.4-1997. Report No. 004898KN, CSR Building Materials Research Centre, 376 Victoria St, Wetherill Park, Sydney, 2000.
9. Young, S.A. and Clancy, P., "Structural Modelling of Light-timber Framed Walls in Fire," *Fire Safety Journal*, Vol. 36, No. 3, 2001, pp. 241–268.
10. Takeda, H. and Mehaffey, J.R., "WALL2D: a Model for Predicting Heat Transfer through Wood-stud Walls Exposed to Fire," *Fire and Materials*, Vol. 22, 1998, pp. 133–140.
11. Young, S.A. and Clancy, P., "Compression Mechanical Properties of Wood at Temperatures Simulating Fire Conditions," *Fire and Materials*, Vol. 25, No. 3, 2001, pp. 83–93.
12. Jong, F. and Clancy, P., "Compression Properties of Wood as Functions of Moisture Stress and Temperature," *Structures in Fire*, Second International Workshop, Christchurch New Zealand, 2002, pp. 223–242.
13. Jong, F. and Clancy, P., "Compression Properties of Wood as Functions of Moisture Stress and Temperature," Special Issue of *Fire and Materials for Structures in Fire*, Second International Workshop, Christchurch New Zealand, in-press.
14. *Standard Methods of Static Tests of Timbers in Structural Sizes*; American Society for Testing Materials and Materials: ASTM D198-84, 1994.
15. White, R.H. and Schaffer, E.L., "Transient Moisture Gradient in Fire-Exposed Wood Slab," *Wood and Fiber*, Vol. 13, Part 1, 1981, pp. 17–38.
16. Fredlund, B., *A Model for Heat and Mass Transfer in Timber Structures During Fire, A Theoretical, Numerical and Experimental Study*, Lund University, Sweden, Institute of Science and Technology, Department of Fire Engineering, Report LUTVDG/(TVBB-1003), 1988.
17. White, R.H., Cramer, S.M. and Shrestha, D.K., *Fire Endurance Model of a Metal-Plate-Connected Wood Truss*, Research Paper FPL 522, US Department of Agriculture, Forest Products Laboratory, Madison, Wisconsin, USA, 1993.
18. Gerhards, C.C., "Effect of Moisture Content and Temperature on the Mechanical Properties of Wood: An Analysis of Immediate Effects," *Wood and Fiber*, 1984, pp. 4–36.
19. ISO 834, "Fire-Resistance Tests- Elements of Building Construction," International Organization for Standardization, CH-1211, Geneva 20, Switzerland.
20. Pettersson, O. and Ödeen, K., Brandteknisk Dimensionering, Stockholm, 1978.
21. König, J., Noren, J., Olesen, F.B., and Hansen, F.T., *Timber Frame Assemblies Exposed to Standard and Parametric Fires, Part 1: Fire Tests*. Trätek (Swedish Institute for Wood Technology Research), Stockholm, Report I 9702015, February, 1997.